Organic & Biomolecular Chemistry

RSC Publishing

PAPER

View Article Online
View Journal | View Issue

Cite this: *Org. Biomol. Chem.*, 2013, **11**, 4232

The chemical fate of paroxetine metabolites. Dehydration of radicals derived from 4-(4-fluorophenyl)-3-(hydroxymethyl)piperidine†

Davor Šakić,[a] Florian Achrainer,[b] Valerije Vrček*[a] and Hendrik Zipse[b]

Received 31st January 2013,
Accepted 1st May 2013

DOI: 10.1039/c3ob40219c

www.rsc.org/obc

Quantum chemical calculations have been used to model reactions which are important for understanding the chemical fate of paroxetine-derived radicals in the environment. In order to explain the experimental observation that the loss of water occurs along the (photo)degradation pathway, four different mechanisms of radical-induced dehydrations have been considered. The elimination of water from the *N*-centered radical cation, which results in the formation of an imine intermediate, has been calculated as the most feasible process. The predicted energy barrier ($\Delta G^{\#}_{298}$ = 98.5 kJ mol^{-1}) is within the barrier limits set by experimental measurements. All reaction intermediates and transition state structures have been calculated using the G3(MP2)-RAD composite procedure, and solvent effects have been determined using a mixed (cluster/continuum) solvation model. Several new products, which comply with the available experimental data, have been proposed. These structures could be relevant for the chemical fate of antidepressant paroxetine, but also for biologically and environmentally related substrates.

Introduction

The antidepressant paroxetine (Paxil®) is an important representative of an emerging group of pharmacologically active phenylpiperidines. It is a selective serotonin reuptake inhibitor (SSRI) that is widely prescribed to treat depression. Recent studies have shown that paroxetine and its metabolites[1–3] have the potential to accumulate in waste waters,[4] but also in the tissue of fish[5] as a result of discharges of this antidepressant into surface waters from municipal wastewater treatment plants.[6,7]

Environmental risk assessment of paroxetine has been performed earlier, but only the parent (3*S*,4*R*)-(4-(4′-fluorophenyl)-3-(3,4-methylenedioxyphenoxymethyl)piperidine (**I**) and its major human metabolite *trans*-4-[4-(4′-fluorophenyl)-3-piperidinylmethoxy]-2-methoxyphenol (**II**) have been considered (Scheme 1) in more detail.[8] According to ecotoxicity results, paroxetine itself should not exert any significant effects on aquatic organisms. From an environmental fate perspective, paroxetine appears to be hydrolytically stable, while irradiation studies did not show any major UV degradants.

Kwon and Armbrust have shown that paroxetine, if exposed to simulated sunlight, easily undergoes hydrolysis and dehydration in the environment, resulting in relatively stable by-product(s).[9] The hydrolyzed photoproduct (3*S*,4*R*)-4-(4-fluorophenyl)-3-(hydroxymethyl)piperidine (**III**) is considered as the main environmental metabolite, whereas the possible dehydrated photoproduct has been designated as **IV** (Scheme 1). It is likely that **IV** was produced by loss of water followed by cyclization, but no mechanistic details have been provided. The only structural information for the dehydrated product is the mass spectrum signal at *m*/*z* 192 $[M + H]^+$, leading to a molecular mass of 191. No environmental risk assessment has been performed for the two respective compounds **III** and **IV**.

We have recently proposed that, along with the hydrolysis **I** → **III**, a number of different rearrangements of paroxetine are feasible if chlorination ($HOCl/Cl_2$) of waste water is taken into account.[10] Chemical transformations of *N*-chlorinated derivative **IIIa** (Scheme 1) have been investigated computationally in water as the reaction medium. In addition to the hydrolyzed product **III**, alternative products have been predicted and suggested as relevant for the chemical fate of paroxetine. In order to provide a more comprehensive picture of reaction possibilities, the rearrangement reactions in the open-shell counterparts of paroxetine metabolites are investigated in this work. While the base-catalyzed reactions in the closed-shell systems occur due to the water chlorination, the paroxetine-derived radicals are generated through photolysis.

[a]*University of Zagreb, Faculty of Pharmacy and Biochemistry, A. Kovačića 1, HR-10000 Zagreb, Croatia. E-mail: valerije@pharma.hr; Fax: +385 1 4856201; Tel: +385 1 6394441*

[b]*Department of Chemistry, LMU München, Butenandtstr. 13, D-81377 München, Germany*

†Electronic supplementary information (ESI) available. See DOI: 10.1039/c3ob40219c

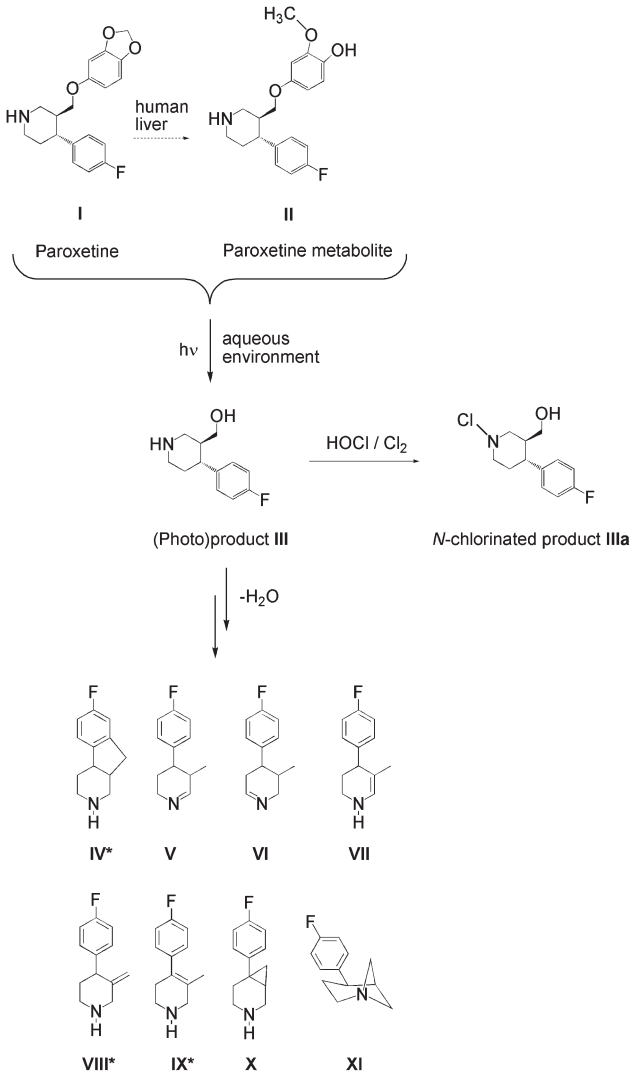

Scheme 1 (Bio)degradation processes of paroxetine and its metabolites. Proposed closed-shell products ($C_{12}H_{14}FN$) of rearrangements in paroxetine derived radicals. Structures reported in earlier studies are designated by an asterisk.

Photodegradation of paroxetine follows first-order kinetics, and the reaction rate constant at pH 7 is 0.0529 h^{-1}.[9] This photodegradation process includes the hydrolysis of **I** to **III** (the experimentally detected photoproduct), and the subsequent rearrangement of **III** to the dehydration product (presumably **IV**). While the hydrolysis results in a single product (**III**), different products may arise from dehydration of **III** (Scheme 1). The experimentally-determined rate constant at pH 7 (calculated as the rate of disappearance of **I**) corresponds to an energy barrier of *ca.* 100 kJ mol^{-1} at 25 °C. The accuracy of this value, which is based on the assumption of a unimolecular process, is not well established and we therefore assume that all processes below or within a bracket of 10 kJ mol^{-1} of the target experimental barrier (shown as a grey band in Fig. 1) contribute to the measured reaction rate.

Based on the computational results presented here we outline conceivable pathways for the formation of the (photo) degradation products observed in the experimental studies of Kwon and Armbrust. The computational results can also help to identify the structures of photoproducts, which have been proposed earlier on the basis of the MS signal only (*m*/*z* 192 $[M + H]^+$). According to other experimental studies, hydrolysis and dehydration of paroxetine can result in several products with a molecular mass of 191.[2,11–13] Therefore, in addition to the photoproduct **IV**, additional structures **V–XI** (Scheme 1) which match the observed MS signal should be considered as possible degradation products of paroxetine.

In order to investigate all feasible pathways in radical-mediated processes and to search for possible products, quantum chemical models are used to calculate energies and geometries of reaction intermediates and transition state structures. Of special importance is to clarify the mechanism of dehydration which seems to be operative in photodegradation of paroxetine derived radicals. Our investigation has been focused on products which have chemical structures consistent with the experimentally observed data. Only processes for which the calculated energy barrier is lower than 200 kJ mol^{-1} have been taken into account (see Fig. 1). It is important to note that if any radical-mediated rearrangement corresponds to the rate-determining step, it should not exceed the barrier limit of *ca.* 100 kJ mol^{-1}, as determined earlier in photolysis experiments.[9]

Four different pathways of dehydration have been considered computationally: (i) the formation of imines **V** and **VI**, and enamine **VII**, (ii) the formation of alkenes **VIII** and **IX**, (iii) cyclodehydration reactions resulting in aza-bicycloheptanes **X** and **XI**, and (iv) the five-membered ring closure in **IV**. A more comprehensive analysis and additional data for all reaction possibilities are deposited in the ESI.† All investigated processes include the dehydration step, which is in accord with the experimental observation that the elimination of a water molecule must occur along the degradation pathway.

A dehydration mechanism has been postulated in chemical transformations of different phenylpiperidine-containing biomolecules.[14–17] Therefore, the comparative study of the competitive processes i–iv is not only relevant for the chemical fate of paroxetine, but may also be relevant for other biologically and environmentally relevant substrates.

Results and discussion

The photolytically induced homolysis[9] of the N–H bond in the (photo)product **III** or the N–Cl bond in the *N*-chlorinated product **IIIa** can result in the formation of *N*-centered radical **1a** (Scheme 2). It has been shown that *N*-chlorinated species are more susceptible to photodegradation, mostly due to the homolytic bond dissociation energy (BDE), which is lower for the N–Cl bond than for the corresponding N–H bond.[18] The ease of formation of *N*-centered radicals has been reported for a series of chloramines, which play an important role in environmental chemistry and biochemistry.[19–23]

Once formed, the *N*-centered radical **1a** can undergo fast protonation yielding the radical cation **1b**. The most stable form of **1b** adopts a chair conformation of the piperidine ring

Published on 01 May 2013.

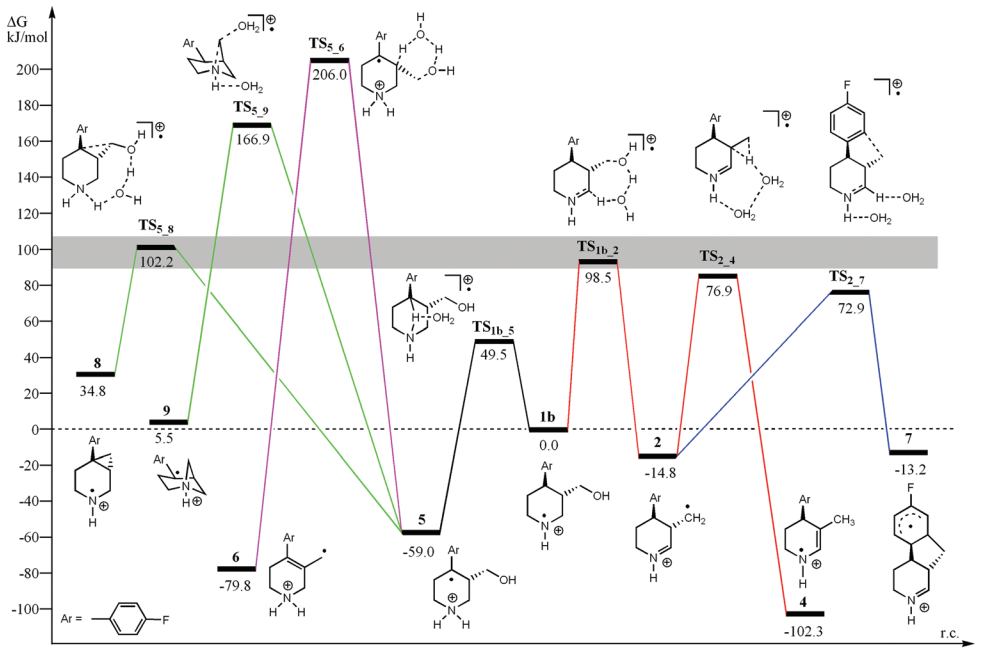

Fig. 1 Schematic energy profile (G3(MP2)-RAD + ΔG_{solv}) for dehydration mechanisms (the formation of imine/enamine (i), red lines; the alkene formation (ii), magenta lines; the formation of azabicycloheptanes (iii), green lines; the five-membered ring closure (iv), blue lines) in radical cations **1b** and **5** derived from the paroxetine metabolite **III** (or **IIIa**). Only the lower energy transition structures for water-assisted processes are presented. The energy of the *N*-centered radical **1b** is set to zero (dashed line). The gray band denotes the target experimental barrier for paroxetine (photo)degradation. Open-shell precursors (Arabic numerals) are connected to their corresponding closed-shell products (Roman numerals).

moiety with both substituents (fluorophenyl and hydroxymethyl) in the equatorial position (the conformer with substituents in the axial position is 11 kJ mol^{-1} less stable if solvation effects are included). The spin density (NPA values) is mainly localized on the nitrogen atom (0.73 au). The calculated pK_a value for **1b** (at the G3(MP2)-RAD + ΔG_{solv} level according to the thermodynamic cycle presented in ESI†) is 6.5, which is similar to the parent piperidine radical (pK_a = 5.8).[24,25] This suggests that both neutral (**1a**) and protonated (**1b**) forms coexist in neutral media. *N*-Centered radicals **1a** and **1b** can undergo a variety of further rearrangements.[26,27]

It is known that protonation of aminyl radicals (such as **1a**) strongly affects the reactivity of these neutral intermediates.[28–31] Therefore, the radical cation **1b** and its rearranged products (see below) have been selected as species relevant for the description of the chemical fate of paroxetine metabolites. For comparison, rearrangements in the neutral aminyl radical **1a** have also been calculated and the corresponding results have been deposited in the ESI.†

Dehydration of 1b with imine/enamine formation

It is known that *N*-centered radical cations may undergo fragmentation reactions, which involve the cleavage of the C$_\alpha$–H bonds.[32] The homolytic cleavage is much easier than in the neutral aminyl radical due to the strong electron withdrawing effect of the positive charge in the protonated form.[33,34]

Therefore, *N*-centered radical cation **1b** is expected to undergo C$_\alpha$–H cleavage in which a hydrogen atom is transferred from either C2 or C6 to the C7-hydroxyl group (numbering defined in Scheme 2). Both pathways were investigated computationally, with the former process being energetically more favorable. The calculated energy barrier $\Delta G^{\#}$ for the intramolecular hydrogen atom transfer from the C2 position is 139.5 kJ mol^{-1} (k_r = 8.10 × 10^{-9} h^{-1}). If one explicit water molecule is included in the calculation, the energy barrier for **1b** → **2** reduces to 98.5 kJ mol^{-1} (k_r = 0.1235 h^{-1}), which is in line with the experimentally determined limit for dehydration reaction (*ca.* 100 kJ mol^{-1} at 298.15 K). The corresponding transition state **TS$_{1b_2}$** is characterized by a seven-membered ring geometry, in which the water molecule assists C2–H cleavage coupled with (C7–O) bond cleavage (Fig. 1). The latter bond is slightly elongated (1.49 Å) as compared to **1b** (1.41 Å) which suggests that the elimination of water occurs simultaneously with the hydrogen atom transfer. Only negligible spin density is located on the migrating hydrogen throughout the reaction (SD(H$_{migr}$) = 0.01 in **TS$_{1b_2}$**), suggesting that spin flows directly from the nitrogen atom in **1b** (0.73 au) to the C7 carbon atom (1.04 au) in **2**.

The iminium radical cation **2** and two water molecules have been located at the product side of the reaction pathway using the IRC procedure. This is a distonic radical in which the positive charge is distributed over the imine moiety (q(C2) = 0.39), while the spin density is localized on the carbon center C7 (1.04 au). According to this result, the structure **V** (the closed-shell analogue of **2**) has been proposed as the dehydration product of the metabolite **III** (or **IIIa**). It represents a conceivable structure with chemical formula (in protonated form: $C_{12}H_{15}FN$) which matches the experimentally observed signal of *m*/*z* 192. The corresponding closed-shell analogue of

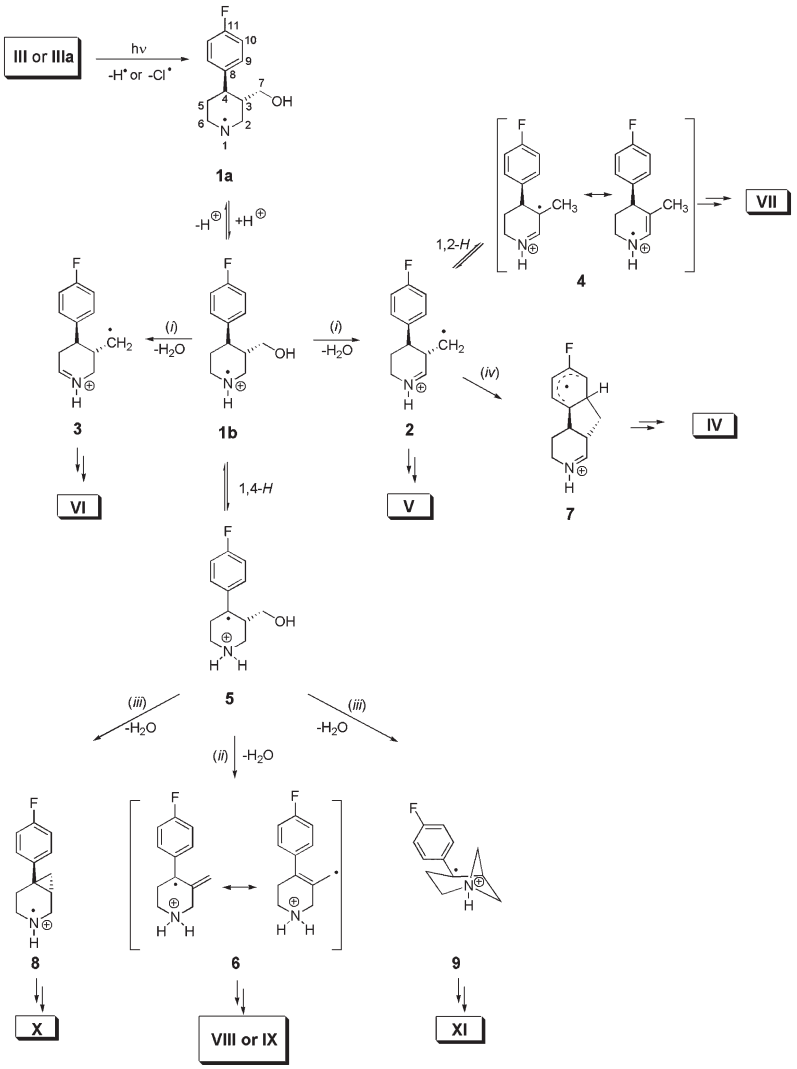

Scheme 2 Proposed dehydration mechanisms (i–iv) in radical cations **1b** and **5** derived from paroxetine metabolites **III** and **IIIa**. Closed-shell reactants/products from Fig. 1 are indicated in boxes. Explicit water molecules coordinated to each radical cation are not presented.

iminium radical cation **3** (structure **VI** in Scheme 1) is predicted to be only a minor product of the dehydration reaction.

The distonic radical cation **2** is more stable by 14.8 kJ mol^{-1} as compared to the *N*-centered radical **1b**. It can undergo further rearrangement through transfer of the C3–H atom to the C7 position. While being forbidden by orbital symmetry conservation rules (the calculated barrier $\Delta G^{\#}$ is over 220 kJ mol^{-1}), this 1,2-hydrogen migration becomes feasible when mediated by water molecules. The transition state structure $\mathbf{TS_{2\_4}}$ for the solvent assisted 1,2-hydrogen migration is calculated to be 91.7 kJ mol^{-1} above the imine **2**, which makes this rearrangement kinetically favorable. The resulting enamine radical **4**, presented in Scheme 2 with two resonance structures, has been calculated as the most stable rearranged product (102.3 kJ mol^{-1} more stable than **1b**). It is characterized by the planar C6–N1–C2–C3 moiety in which the spin is distributed between N1 (0.40 au) and C3 (0.60 au) atoms. Its closed-shell form corresponds to the structure **VII** in Scheme 1.

Imines such as **V** and **VI**, and enamines such as **VII** may easily undergo hydrolysis giving the expected products with free amino and aldehyde functionalities.[23,35,36] None of these products, however, can be assigned to the observed signal in the mass spectrum.[37]

Dehydration of 5 with alkene formation

The two alkene products **VIII** and **IX** (Scheme 1) have been observed in elimination reactions of paroxetine metabolites.[12,38] The existence of **VIII** as an intermediate in the degradation of **III** has also been confirmed by using electrospray ionization mass spectrometry (ESI-MS).[11] In our quest for the possible dehydration product, the alkenes **VIII** and **IX** have been targeted as structures with chemical formula matching the experimentally observed signal (*m*/*z* 192). The most favorable pathway which precedes the formation of **VIII** and **IX** corresponds to the loss of water from carbon-centered radical cation **5**. Radical cation **5** is a distonic form of the *N*-centered radical **1b** (charge and radical sites are spatially separated in **5**),

and is calculated to be 59.0 kJ mol^{-1} more stable than the latter. The unpaired spin in **5** is localized on the C4 carbon atom (0.74 au) with some flow to carbon centers C9 (0.22 au) and C11 (0.21 au) in the phenyl ring. It is formed by the 1,4-[N↔C]-hydrogen migration **1b** → **5** *via* transition structure **TS$_{1b_5}$**. In this transition structure the water molecule is bound to the migrating hydrogen (complex of type $H_{migr}\cdots OH_2$ in Fig. 1). Analysis of partial charge (NPA values) and spin distribution along the 1,4-[N↔C]-H migration reveals that the migrating hydrogen carries a positive charge throughout the reaction ($q(H_{migr})$ = 0.48 e in **TS$_{1b_5}$**). Simultaneously, only the negligible spin density is located on the H_{migr} (0.02 au). The calculated energy barrier for this intramolecular H-shift is 106.3 kJ mol^{-1} ($k_r = 5.33 \times 10^{-3}$ h^{-1}), or 49.5 kJ mol^{-1} (k_r = 0.4752 h^{-1}) with one explicit water added to the system.

The transition state structure **TS$_{5_6}$** (Fig. 1), which connects radical cation **5** and the alkene product **6**, is located 206.0 kJ mol^{-1} ($k_r = 1.81 \times 10^{-20}$ h^{-1}) above the starting radical cation **1b**. Radical cation **6** can undergo further transformations to yield the closed-shell alkenes **VIII** or **IX**, the latter of which is more stable on thermochemical grounds.[12] However, the calculated energy barrier for **5** → **6** exceeds the experimentally measured value of 100 kJ mol^{-1}, which makes this dehydration process kinetically less favorable.

Cyclodehydration reactions of 5

The elimination of water from radical cation **5** can also be coupled to the formation of 3- or 4-membered ring systems. In the cyclodehydration reaction **5** → **8** the simultaneous elimination of the C7-hydroxyl group and the hydrogen atom from the N1 position results in the formation of the azabicycloheptane product **8**. The calculated energy barrier for this cyclopropanation reaction amounts to 161.2 kJ mol^{-1} ($k_r = 1.28 \times 10^{-11}$ h^{-1}) if one explicit water is added, which is substantially lower than the barrier for the formation of alkene radical cation **6** (see above). The radical cation product **8** can subsequently be transformed into the closed-shell parent **X**, which has already been targeted as a bioactive lead compound.[39,40] It is closely related to paroxetine as the azabicycloheptane derivatives have been recently designed as potent and selective triple reuptake inhibitors,[41,42] and the same heterocyclic moiety has been described as important in monoamine oxidase substrates.[43]

The cyclodehydration pathway **5** → **9** couples the elimination of water to the formation of an azetidine ring system (Scheme 2). The dehydration reaction with azetidine ring closure occurs in a number of pharmaceuticals based on aminoalcohol substructures,[44–46] including the tropane-derived paroxetine analogs,[47] which supports the proposal that a similar mechanism can be expected in the paroxetine metabolite **III**. The calculated energy barrier for **5** → **9** is 64.7 kJ mol^{-1} higher than the corresponding barrier for cyclodehydration **5** → **8**. This is in line with earlier studies showing that the energy barrier for azetidine ring formation in aminoalcohols[48] or aminohalides[49] can be quite substantial (up to 200 kJ mol^{-1}).

Dehydration of 1b with five-membered ring formation

Cyclization reactions are also conceivable starting from radical cation **2** and then involve formal radical attack at the aromatic ring system to yield tricyclic radical cation **7**. This is a distonic radical in which the positive charge is distributed over the imine moiety (q(C2) = 0.40 e), while the spin density is delocalized over the carbon centers C8 (0.41 au), C10 (0.44 au) in the phenyl ring. Radical addition reactions to aromatic ring systems are generally considered to be thermochemically unfavourable processes, but it should be added that intramolecular radical addition to a benzene ring system has recently been reported for fibrate pharmaceuticals in the context of environmental degradation processes.[50] The calculated energy barrier for the process **2** → **7** is 87.7 kJ mol^{-1} (k_r = 9.72 h^{-1}), which is within the barrier limits set by experimental measurements. The respective transition state structure **TS$_{2_7}$** (Fig. 1) is characterized by one imaginary frequency (544*i* cm^{-1}), which corresponds to the ring closure process. In this structure the calculated distance between C7 and C9 carbon atoms is only 2.1 Å. The spin density distribution indicates that the spin is considerably delocalized from the C7 carbon atom (0.63 au) to carbon centers C8 (0.28 au), C9 (0.18 au), and C10 (0.27 au) in the phenyl ring. The calculated energies of the ground states suggest that the reaction **2** → **7** is slightly endergonic. However, the reaction can proceed if the following energy barrier for rearrangements of **7** is low and the final product is lower in energy than reactant **2**. In order to transform radical cation **7** into the closed-shell product **IV**, the rearomatization of the attacked ring systems and subsequent electron transfer steps are required.

Conclusions

In this work we have compared the reaction energetics for several dehydration processes which can occur in radical cations generated by photolysis of the paroxetine metabolite **III** (or **IIIa**). The barrier value of *ca.* 100 kJ mol^{-1} (at 298.15 K) has been determined earlier by experimental measurements in which paroxetine has been exposed to simulated sunlight and kinetic parameters (k_r = 0.0529 h^{-1}) of photodegradation have been measured spectrophotometrically.[9] It corresponds to the estimated half-life of 13.1 h, indicating that the paroxetine metabolite is not persistent to photolysis in water (pH = 7). However, the photoproduct is stable under photolytic conditions, and therefore a search for the mechanism of its formation is of environmental relevance. All reaction possibilities, for which the calculated barrier noticeably exceeds the limit set by the experiment, are deposited in the ESI.†

Only the *N*-centered radical cation **1b** and its distonic form **5** have been considered as important reactive intermediates. The former is the free radical formed directly from the paroxetine metabolite **III** (or **IIIa**), while the latter is the most stable distonic isomer. Both species **1b** and **5** are interconnected *via* the structure **TS$_{1b_5}$** which represents the transition state for the corresponding 1,4-hydrogen migration ($\Delta G^{\#}$ = 49.5 kJ mol^{-1};

k_r = 0.4752 h^{-1}). Two different rearrangements in the radical cation **1b** can be distinguished (Scheme 2): the elimination of water resulting in imine **2** and enamine **4** formation (i) and the cyclization of the initially formed imine giving structure **7** (iv). As well, the radical cation **5** can undergo two dehydration reactions: the elimination of water resulting in the formation of alkene **6** (ii) and cyclodehydration in which azabicycloheptanes **8** and **9** are formed (iii).

The elimination of water from the starting radical **1b** has been calculated as the most important reaction channel ($\Delta G^{\#}$ = 98.5 kJ mol^{-1}; k_r = 0.1235 h^{-1}) leading to the formation of iminium radical cation **2**. The latter species can be easily transformed into enamine **4** (the most stable intermediate on the potential energy surface investigated) or converted to **7** by an intramolecular cyclization. The latter intermediate is an open-shell precursor for the parent structure **IV**, which has been proposed earlier as a possible photoproduct of the paroxetine degradation in water.[9] In contrast, the parent enamine **VII**, derived from intermediate **4**, has not been considered as a conceivable product. We have shown here that, in both cases, the imine radical **2** is the key intermediate for the formation of the photoproducts **IV** and **VII**.

In addition, two cyclodehydration mechanisms (iii) have been considered: the concerted one in which the cyclopropane ring has been formed simultaneously with the elimination of water, and the stepwise mechanism in which formation of the four-membered azetidine moiety occurs after the elimination of water. The calculated barriers for both reactions are relatively high, with the former reaction **5** → **8** being the more favorable process.

The dehydration process (ii), which results in the formation of alkene radical **6**, has been found to exceed the targeted barrier limit of *ca.* 100 kJ mol^{-1}. Although the formation of the parent alkene products **VIII** and **IX** from paroxetine metabolites has been detected experimentally,[12,38] these reactions most likely proceed without the intermediacy of free radicals.

The calculated barriers for all dehydration reactions starting from structure **5**, which occur prior to the formation of the closed-shell parents **VIII**, **IX**, **X** and **XI**, are relatively high. Therefore, these structures are unlikely candidates to explain the experimental results. However, they could be important in understanding the chemical fate of other environmentally relevant compounds which are structurally related to paroxetine (*i.e.* containing the phenyl-piperidine and/or aminoalcohol groups). It is known that the dehydration process is important for the metabolic and environmental fate of a series of pharmaceuticals and other biologically relevant compounds, which contain aminoalcohol moieties ($R_2N(CH_2)_nOH$, where n = 2–4). For example, haloperidol, the most widely used drug for the treatment of neuropsychiatric disorders, undergoes dehydration; it has been shown that dehydration is the first reaction step in the bioactivation[14] and electrochemical oxidation of haloperidol.[16] A similar dehydration mechanism has been postulated in the transformation of selective inhibitors of serine proteases[15] and the central nervous system stimulant pipradrol.[17]

In conclusion, quantum-chemistry models have been employed in a search for products of radical-mediated photodegradation of paroxetine. Several structures, not considered earlier, have been located, and the reaction mechanisms underlying their formation have been described. We propose structures **IV**, **V**, **VI**, and **VII** (Scheme 1) as probable photoproducts which fit to available experimental data.

Computational details

DFT calculations are employed for geometry optimizations and frequency calculations for open-shell systems at the unrestricted UB3LYP/6-31G(d) level.[51] Thermal corrections to Gibbs energies have been calculated at the same level of theory using the rigid rotor/harmonic oscillator model. All energies are reported at 298.15 K. Improved energetics have been calculated using the double hybrid B2K-PLYP/6-311+G(3df,2p)[52] and B2-PLYP/aug-def2-TZVPP methods,[53] which combine exact HF exchange with an MP2-like correlation to a DFT calculation (the corresponding energies are included in ESI†). It has been found that B2K-PLYP shows an excellent performance for calculating barrier heights for water-catalyzed proton-transfer reactions,[54] and radical reactions.[55,56] The B2-PLYP method has recently been successfully benchmarked against the G3B3 composite model.[10] Finally, we use the G3(MP2)-RAD composite model[57] as our reference procedure in order to evaluate the efficiency of DFT methods. Only the G3(MP2)-RAD energies are reported throughout the text (calculated energies are relative to separated reactants). The (U)CCSD(T)/6-31G(d) calculations for the G3(MP2)-RAD model have been performed with MOLPRO 2006.1,[58] while all other quantum mechanical calculations have been performed with Gaussian 09.[59]

The calculated energy barriers ($\Delta G^{\#}$, in kJ mol^{-1}) are converted to reaction rate constants (k_r, in h^{-1}) throughout the text. However, these estimates are rather approximate. A difference in Gibbs energy of activation of 5.7 kJ mol^{-1} (at 298.15 K) results in a reaction rate difference of one order of magnitude. Therefore, some caution must be exercised in the interpretation of absolute values for the predicted reaction rate constants, whereas the relative numbers are more reliable. The corresponding half-life predictions are also sensitive to errors in the calculation of $\Delta G^{\#}$, which prevents an exact assessment of the persistence of metabolites.

Analytical vibrational analysis was performed to characterize each stationary point as a minimum (number of imaginary frequencies = 0) or a first-order saddle point (number of imaginary frequencies = 1). Intrinsic reaction coordinate (IRC) calculations were performed at the corresponding level of theory to identify the minima connected through the transition state. The initial geometries used were those of the corresponding transition state structures, and the paths were followed in both directions from that point. This method verified that a given transition structure indeed connected the presumed energy minimum structures.[60]

Gibbs energies of solvation have been determined using the CPCM continuum solvation model at the UB3LYP/6-31G(d) level, with UAKS atomic radii and the electrostatic scaling factor (alpha value) set to 1.2 for all atoms. The solvent relative permittivity of ε = 78.4 (water) was used. To correctly describe open-shell systems in water the inclusion of bulk and specific solvent effects is mandatory. We have found that the addition of one explicit water molecule substantially lowers the calculated energy barriers for all processes investigated. The number of explicit water molecules (n = 0–3) is varied in order to identify the most stable structure, *i.e.* to obtain the most negative Gibbs energy of solvation. We have found that one water molecule is "the ideal number of solvent molecules"[61] for all structures involved in selected processes depicted in Fig. 1 (see details in ESI†). The addition of the second and the third water molecule is not favorable in Gibbs energy terms. Therefore, all structures and relative energies reported throughout the text include one extra water molecule. The most stable forms of water-complexed species are located by placing water molecules in a variety of locations to sample the different arrays of interaction networks available between the corresponding free radical and water. Initial configurations were created using a locally modified version of the stochastic search method.[62–64]

Different mechanisms for water-catalyzed reactions (denoted as A, B, or C in ESI†) have been considered,[65] but only the most favorable are presented in the text (for selected examples see Fig. 1).

Published on 01 May 2013.

Acknowledgements

The financial support by Alexander von Humboldt Foundation (a research group linkage project "Computational Life Sciences on Open Shell Intermediates") is gratefully acknowledged. We thank the Computing Centre SRCE of the University of Zagreb for allocating computer time on the Isabella cluster where a part of the calculations was performed.

Notes and references

1 S. X. Zhao, D. K. Dalvie, J. M. Kelly, J. R. Soglia, K. S. Frederick, E. B. Smith, R. S. Obach and A. S. Kalgutkar, *Chem. Res. Toxicol.*, 2007, **20**, 1649.
2 M. Segura, J. Ortuno, M. Farre, R. Pacifici, S. Pichini, J. Joglar, J. Segura and R. de la Torre, *Rapid Commun. Mass Spectrom.*, 2003, **17**, 1455.
3 P. Massaroti, N. M. Cassiano, L. F. Duarte, D. R. Campos, M. A. M. Marchioretto, G. Bernasconi, S. Calafatti, F. A. P. Barros, E. C. Meurer and J. Pedrazzoli, *J. Pharm. Pharm. Sci.*, 2005, **8**, 340.
4 T. Vasskog, T. Anderssen, S. Pedersen-Bjegaard, R. Kallenborn and E. Jensen, *J. Chromatogr. A*, 2008, **1185**, 194.
5 S. Chu and C. D. Metcalfe, *J. Chromatogr. A*, 2007, **1163**, 112.
6 C. D. Metcalfe, S. Chu, C. Judt, H. Li, K. D. Oakes, M. R. Servos and D. M. Andrews, *Environ. Toxicol. Chem.*, 2010, **29**, 79.
7 M. Gros, M. Petrović and D. Barcelo, *Anal. Chem.*, 2009, **81**, 898.
8 V. L. Cunningham, D. J. Constable and R. E. Hannah, *Environ. Sci. Technol.*, 2004, **38**, 3351.
9 J. W. Kwon and K. L. Armbrust, *Environ. Toxicol. Chem.*, 2004, **23**, 1394.
10 D. Sakic, H. Zipse and V. Vrcek, *Org. Biomol. Chem.*, 2011, **9**, 4336.
11 W. F. Smyth, J. C. Leslie, S. McClean, B. Hannigan, H. P. McKenna, B. Doherty, C. Joyce and E. O'Kane, *Rapid Commun. Mass Spectrom.*, 2006, **20**, 1637.
12 H. Navratilova, Z. Kriz and M. Potacek, *Synth. Commun.*, 2004, **34**, 2101.
13 W. M. A. Niessen, *Mass Spectrom. Rev.*, 2011, **30**, 626.
14 J. Fang and J. W. Gorrod, *Toxicol. Lett.*, 1991, **59**, 117.
15 J. Kotthaus, T. Steinmetzer, J. Kotthaus, D. Schade, A. Van De Locht and B. Clement, *Xenobiotica*, 2010, **40**, 93.
16 T. J. Mali'n, L. Weidolf, N. Castagnoli Jr. and U. Jurva, *Rapid Commun. Mass Spectrom.*, 2010, **24**, 1231.
17 J. Z. Long, X. Jin, A. Adibekian, W. Li and B. F. Cravatt, *J. Med. Chem.*, 2010, **53**, 1830.
18 R. J. O'Reilly, A. Karton and L. Radom, *J. Phys. Chem. A*, 2011, **115**, 5496.
19 D. I. Pattison, M. J. Davies and K.-D. Asmus, *J. Chem. Soc., Perkin Trans. 2*, 2002, 1461.
20 D. I. Pattison, R. J. O'Reilly, O. Skaff, L. Radom, R. F. Anderson and M. J. Davies, *Chem. Res. Toxicol.*, 2011, **24**, 371.
21 H. Zhang and C.-H. Huang, *Environ. Sci. Technol.*, 2005, **39**, 4474.
22 C. L. Hawkins and M. J. Davies, *Chem. Res. Toxicol.*, 2002, **15**, 83.
23 X. L. Armesto, M. L. Canle, M. V. Garcia and J. A. Santaballa, *Chem. Soc. Rev.*, 1998, **27**, 453.
24 V. Vrcek and H. Zipse, *J. Org. Chem.*, 2009, **74**, 2947.
25 H. K. Hall, *J. Am. Chem. Soc.*, 1957, **79**, 5441.
26 S. Hammerum and C. B. Nielsen, *J. Phys. Chem. A*, 2005, **109**, 12046.
27 I. Janovsky, W. Knolle, S. Naumov and F. Williams, *Chem.–Eur. J.*, 2004, **10**, 5524.
28 J. W. Gauld and L. Radom, *J. Am. Chem. Soc.*, 1998, **119**, 9831.
29 B. D. Wagner, G. Ruel and J. Lusztyk, *J. Am. Chem. Soc.*, 1996, **118**, 13.
30 D. Moran, R. Jacob, G. P. F. Wood, M. L. Coote, M. J. Davies, R. A. J. O'Hair, C. J. Easton and L. Radom, *Helv. Chim. Acta*, 2006, **89**, 2254.
31 O. M. Musa, J. H. Horner, H. E. Shahin and M. Newcomb, *J. Am. Chem. Soc.*, 1996, **118**, 3862.
32 E. Baciocchi, M. Bietti and O. Lanzalunga, *J. Phys. Org. Chem.*, 2006, **19**, 467.

33 S. F. Nelsen and J. T. Ippoliti, *J. Am. Chem. Soc.*, 1986, **108**, 4879.
34 R. D. Burton, M. D. Bartberger, Y. Zhang, J. R. Eyler and K. S. Schanze, *J. Am. Chem. Soc.*, 1996, **118**, 5655.
35 R. W. Fitch, G. D. Sturgeon, S. R. Patel, T. F. Spande, H. M. Garraffo, J. W. Daly and R. H. Blaauw, *J. Nat. Prod.*, 2009, **72**, 243.
36 P. Y. Sollenberger and R. B. Martin, *J. Am. Chem. Soc.*, 1970, **92**, 4261.
37 A referee has correctly noted that products with free amino and aldehyde groups could easily dehydrate under the analytical conditions to give the observed signal of *m*/*z* 192.
38 M. Engelstoft and J. B. Hansen, *Acta Chem. Scand.*, 1996, **50**, 164.
39 I. V. Efremov, B. N. Rogers, A. J. Duplantier, L. Zhang, Q. Zhang, N. S. Maklad, E. V. Evrard and M. A. Brodney, *Wo* 2008012623, 2008.
40 L. Schwink, S. Stengelin, M. Gossel, T. Boehme, G. Hessler, P. Stahl and D. Gretzke, *Wo* 2004072025, 2004.
41 F. Micheli, L. Arista, B. Bertani, S. Braggio, A. M. Capelli, S. Cremonesi, R. Di-Fabio, G. Gelardi, G. Gentile, C. Marchioro, A. Pasquarello, S. Provera, G. Tedesco, L. Tarsi, S. Terreni, A. Worby and C. Heidbreder, *J. Med. Chem.*, 2010, **53**, 7129.
42 F. Micheli, P. Cavanni, D. Andreotti, R. Arban, R. Benedetti, B. Bertani, M. Bettati, L. Bettelini, G. Bonanomi, S. Braggio, R. Carletti, A. Checchia, M. Corsi, E. Fazzolari, S. Fontana, C. Marchioro, E. Merlo-Pich, M. Negri, B. Oliosi, E. Ratti, K. D. Read, M. Roscic, I. Sartori, S. Spada, G. Tedesco, L. Tarsi, S. Terreni, F. Visentini, A. Zocchi, L. Zonzini and R. Di Fabio, *J. Med. Chem.*, 2010, **53**, 4989.
43 P. Bissel, A. Khalil, J. M. Rimoldi, K. Igarashi, D. Edmondson, A. Millera and N. Castagnoli Jr., *Bioorg. Med. Chem.*, 2008, **16**, 3557.
44 V. H. Wysocki, D. J. Burinsky and R. G. Cooks, *J. Org. Chem.*, 1985, **50**, 1287.
45 F. Xu, B. Simmons, R. A. Reamer, E. Corley, J. Murry and D. Tschaen, *J. Org. Chem.*, 2008, **73**, 312.
46 M. J. Galmier, B. Bouchon, J. C. Madelmont, F. Mercier, F. Pilotaz and C. Lartigue, *J. Pharm. Biomed. Anal.*, 2005, **38**, 790.
47 S. P. Runyon, J. P. Burgess, P. Abraham, K. I. Keverline-Frantz, J. Flippen-Anderson, J. Deschamps, A. H. Lewin, H. A. Navarro, J. W. Boja, M. J. Kuhar and F. I. Carroll, *Bioorg. Med. Chem.*, 2005, **13**, 2439.
48 G. Bouchoux, N. Choret, F. Berruyer-Penaud and R. Flammang, *Int. J. Mass Spectrom.*, 2002, **217**, 195.
49 S. Stanković, S. Catak, M. D'hooghe, H. Goossens, K. Abbaspour Tehrani, P. Bogaert, M. Waroquier, V. Van Speybroeck and N. De Kimpe, *J. Org. Chem.*, 2011, **76**, 2157.
50 B. Razavi, W. Song, W. J. Cooper, J. Greaves and J. Jeong, *J. Phys. Chem. A*, 2009, **113**, 1287.
51 J. Tirado-Rives and W. L. Jorgensen, *J. Chem. Theory Comput.*, 2008, **4**, 297.
52 A. Tarnopolsky, A. Karton, R. Sertchook, D. Vuzman and J. M. L. Martin, *J. Phys. Chem. A*, 2008, **112**, 3.
53 F. Neese, T. Schwabe and S. Grimme, *J. Chem. Phys.*, 2007, **126**, 124115.
54 See the benchmark study: A. Karton, R. J. O'Reilly and L. Radom, *J. Phys. Chem. A*, 2012, **116**, 4211.
55 B. Chan, R. J. O'Reilly, C. J. Easton and L. Radom, *J. Org. Chem.*, 2012, **77**, 9807.
56 B. Chan and L. Radom, *J. Phys. Chem. A*, 2012, **116**, 3645.
57 L. A. Curtiss, K. Raghavachari, P. C. Redfern, V. Rassolov and J. A. Pople, *J. Chem. Phys.*, 1998, **109**, 7764.
58 MOLPRO, version 2006.1, a package of *ab initio* programs written by H.-J. Werner, P. J. Knowles, G. Knizia, F. R. Manby, M. Schütz, P. Celani, T. Korona, R. Lindh, A. Mitrushenkov, G. Rauhut, K. R. Shamasundar, T. B. Adler, R. D. Amos, A. Bernhardsson, A. Berning, D. L. Cooper, M. J. O. Deegan, A. J. Dobbyn, F. Eckert, E. Goll, C. Hampel, A. Hesselmann, G. Hetzer, T. Hrenar, G. Jansen, C. Köppl, Y. Liu, A. W. Lloyd, R. A. Mata, A. J. May, S. J. McNicholas, W. Meyer, M. E. Mura, A. Nicklaß, D. P. O'Neill, P. Palmieri, K. Pflüger, R. Pitzer, M. Reiher, T. Shiozaki, H. Stoll, A. J. Stone, R. Tarroni, T. Thorsteinsson, M. Wang and A. Wolf, see http://www.molpro.net
59 M. J. Frisch, G. W. Trucks, H. B. Schlegel, G. E. Scuseria, M. A. Robb, J. R. Cheeseman, G. Scalmani, V. Barone, B. Mennucci, G. A. Petersson, H. Nakatsuji, M. Caricato, X. Li, H. P. Hratchian, A. F. Izmaylov, J. Bloino, G. Zheng, J. L. Sonnenberg, M. Hada, M. Ehara, K. Toyota, R. Fukuda, J. Hasegawa, M. Ishida, T. Nakajima, Y. Honda, O. Kitao, H. Nakai, T. Vreven, J. A. Montgomery Jr., J. E. Peralta, F. Ogliaro, M. Bearpark, J. J. Heyd, E. Brothers, K. N. Kudin, V. N. Staroverov, R. Kobayashi, J. Normand, K. Raghavachari, A. Rendell, J. C. Burant, S. S. Iyengar, J. Tomasi, M. Cossi, N. Rega, J. M. Millam, M. Klene, J. E. Knox, J. B. Cross, V. Bakken, C. Adamo, J. Jaramillo, R. Gomperts, R. E. Stratmann, O. Yazyev, A. J. Austin, R. Cammi, C. Pomelli, J. W. Ochterski, R. L. Martin, K. Morokuma, V. G. Zakrzewski, G. A. Voth, P. Salvador, J. J. Dannenberg, S. Dapprich, A. D. Daniels, Ö. Farkas, J. B. Foresman, J. V. Ortiz, J. Cioslowski and D. J. Fox, *GAUSSIAN 09 (Revision A.1)*, Gaussian, Inc., Wallingford CT, 2009.
60 C. Gonzales and H. B. Schlegel, *J. Phys. Chem.*, 1990, **94**, 5523.
61 J. R. Pliego Jr., *Chem. Phys.*, 2004, **306**, 273.
62 M. Saunders, *J. Comput. Chem.*, 2004, **25**, 621.
63 D. Sakic and V. Vrcek, *J. Phys. Chem. A*, 2012, **116**, 1298.
64 V. Vrcek, O. Kronja and M. Saunders, *J. Chem. Theory Comput.*, 2007, **3**, 1223.
65 J. W. Gauld, H. Audier, J. Fossey and L. Radom, *J. Am. Chem. Soc.*, 1996, **118**, 6299.